Design of a Novel Two-Component Hybrid Dermal Scaffold for the Treatment of Pressure Sores.

Vaibhav Sharma, Nupur Kohli, Dale Moulding, Halimat Afolabi, Lilian Hook, Chris Mason, Elena García-Gareta*.

Dr. V. Sharma, Dr. N. Kohli,D H. Afolabi, Dr. L. Hook and Dr. E. García-Gareta

Regenerative Biomaterials Group, RAFT Institute of Plastic Surgery, Mount Vernon Hospital, Northwood, HA6 2RN, UK.

Dr. V. Sharma, Prof. C. Mason

Department of Biochemical Engineering, University College London, Gower Street, London, WC1E 6BT, UK.

Dr. D. Moulding

UCL Great Ormond Street, Institute of Child Health, University College London, 30 Guilford Street, London, WC1N 1EH, UK.

*Corresponding Author:

Dr Elena García-Gareta

RAFT Institute of Plastic Surgery

Leopold Muller Building

Mount Vernon Hospital

Northwood HA6 2RN

United Kingdom

Tel number: + 44 (0) 1923 844 555 / e-mail: garciae@raft.ac.uk

Abstract

The aim of our study was to design a novel two-component hybrid scaffold using the fibrin/alginate porous hydrogel Smart Matrix® combined to a backing layer of plasma polymerised polydimethylsiloxane (Sil) membrane to make the fibrin-based dermal scaffold more robust for the treatment of the clinically challenging pressure sores. A design criteria was established, according to which the Sil membranes were punched to avoid collection of fluid underneath. Manual peel test showed that native silicone did not attach to the fibrin/alginate component while the plasma polymerised silicone membranes were firmly bound to fibrin/alginate. Structural characterisation showed that the fibrin/alginate matrix was intact after addition of the Sil membrane. By adding a Sil membrane to the original fibrin/alginate scaffold the resulting two-component scaffolds had a significantly higher shear or storage modulus G'. *In vitro* cell studies showed that dermal fibroblasts remained viable, proliferated and infiltrated the two-component hybrid scaffolds during the culture period. Our results show that the design of a novel two-component hybrid dermal scaffold was successful according to our proposed design criteria. To the best of our knowledge, this is the first study that reports combination of a fibrin-based scaffold with a plasma-polymerised silicone membrane.

1. Introduction

Chronic pressure sores are challenging wounds which do not progress through the wound healing paradigm and are stuck in one of the healing phases. They are estimated to consume a major portion of the world healthcare budget and resources.[1] In the UK alone, the occurrence of pressure sores has been estimated to be around 1 in a 100 people, costing approximately £400 million per annum. The prevalence of pressure sores has been shown to increase with age and is more common in women.[2,3] These wounds affect localised areas usually over a bony prominence e.g. the lower back and the buttocks, which are subjected to high pressure, shear and/or friction.[4] Similarly, pressure sores also affect amputees at the stump-socket interface, impacting the quality of life for these patients.[5,6] The current therapies to treat pressure sores, include debridement, controlling infection, compression bandages and negative pressure therapy to facilitate healing, and surgical intervention which are costly and ineffective in terms of healing the wound.[7] Therefore, these wounds present a major clinical challenge due to the lack of effective therapies and the continuing rise in the average age of the population.[8]

Over the years, biomaterials have demonstrated a great potential in the treatment of full thickness skin wounds.[8,9] Modern tissue engineering principles involve designing biodegradable three-dimensional (3D) porous scaffolds that allow cell infiltration and diffusion of nutrients and oxygen. In addition to this, for the treatment of pressure sores the tissue-engineered scaffolds should be able to withstand pressure, shear and/or friction when applied on areas such as the lower back and buttocks.[10] Over the years, a range of scaffolds has been designed for the treatment of pressure sores either for use by themselves or as carriers for various components (growth factors, bioactive molecules and different types of cells) into the wound site. These scaffolds can be naturally derived from autologous and cadaveric sources or be synthetically manufactured.[11] Natural protein-based polymers such as fibrin or collagen are widely used as scaffold materials due to enhanced biocompatibility and bioactive properties. In order to improve their mechanical properties they are usually combined with synthetic polymers to form composites.[12-15]

Silicones ($[R_2SiO]_n$; where R represents organic groups such as methyl, ethyl, or phenyl), also known as polymerized siloxanes or polysiloxanes, are synthetic polymers widely used in the biomedical field as solid support (in various shapes) with different bioactive materials (e.g. proteins, nucleic acids) immobilized on the surfaces.[16-18] Their first documented use as a bio-implant was by Lahey in 1946 who developed elastomeric silicone 'bouncing clay' to facilitate bile duct repair and stated that "it is flexible, it will stretch, it will bounce

like rubber and it can be cast in any shape",[19] ideal properties for an implant. In addition to medical devices including pacemakers and catheter components,[20] silicones are also utilised in a variety of pharmaceutical applications including drug delivery systems.[21,22] Although silicones offer excellent strength and ductility, they are bioinert due to their physiochemical and morphological nature.[23] However, polymeric surfaces including silicones can be modified to introduce specific functional groups such as amine, imine, carboxyl, hydroxyl, isocyanate and expoxy, which facilitate the immobilization of biomacromolecules, e.g. proteins, and the interaction of the resulting surfaces with cells. Monomers can be bound onto polymeric surfaces under the influence of plasma through a relatively simple one-step coating process called plasma polymerization.[24-26]

When designing hybrid composites of protein-based and synthetic polymers it is important to maintain the overall biocompatibility of the composite with the target tissue but also between the two different polymers to improve the overall efficiency of the biomaterial.[14,27] In our previous research we developed a 3-step method based on a quick, sensitive and robust immuno-based assay to determine the interfacial binding strength of proteins on synthetic polymeric surfaces.[28] Results using different plasma polymerised silicone surfaces – poly(acrylic acid) and poly(allylamine)- showed that fibrinogen bound with a stronger affinity to plasma polymerised surfaces than to the native silicone.[28] Finally, a simple *in vitro* 2D cell culture model confirmed the biocompatibility of the plasma polymerised silicone surfaces.[28]

Over the past decade our laboratory has developed a novel dermal replacement scaffold composed mainly of fibrin with alginate as a filler component.[29,30] The scaffold is branded Smart Matrix® and is at the commercialisation stage for the treatment of acute full thickness skin wounds such as third degree burns or acute surgical wounds. Smart Matrix® is a porous hydrogel that possesses an open, interconnected porous structure with a micro-pore size distribution ideal for skin regeneration.[29] Moreover, the material behaves like a viscoelastic solid, like skin and dermis tissues, and presents nano-features.[29] *In vitro* cell studies suggest that a higher influx of cells, reduced wound contraction and less scarring would be observed *in vivo* for Smart Matrix® when compared to similar acellular commercially available dermal scaffolds, namely Integra® and Matriderm®.[30]

The aim of this study was to design a novel two-component hybrid scaffold using the fibrin-based dermal replacement scaffold Smart Matrix® with plasma polymerised polydimethylsiloxane (Sil) membrane as a

backing to make the fibrin-based scaffold more robust for the treatment of pressure sores. Plasma polymerization was used to add specific functional groups to the otherwise bioinert Sil. Acrylic acid and allylamine were used as monomers to generate thin layers rich in carboxyl (-COOH) and amine (-NH$_2$) groups making the Sil surface highly branched and cross-linked, to facilitate the immobilization of biomacromolecules (fibrin and alginate in this study) and improve their adherence onto solid surfaces. The design criteria were: 1) Sil membranes should be punched to avoid collection of fluid underneath the membrane which could lead to oedema *in vivo*, 2) the Sil membrane should be firmly bound to the fibrin/alginate component, 3) the thickness of the two-component hybrid scaffolds should not be significantly greater than that of the fibrin/alginate scaffold, 4) the open and interconnected porous structure of the fibrin/alginate component should be maintained after adding the Sil membrane, 5) addition of a Sil membrane should significantly increase the shear modulus of elasticity (G') compared to that of the fibrin/alginate component, 6) cell viability and growth properties on the hybrid scaffolds should be similar to those on the fibrin/alginate component, and 7) cell ingress and integration on the hybrid scaffold should be similar to those on the fibrin/alginate component. The overall hypothesis of this study was that addition of a plasma polymerised Sil membrane to the fibrin/alginate scaffold will add strength to the scaffold without affecting the architecture of the fibrin/alginate component and its cellular properties.

2. Experimental Section

2.1 Scaffold manufacture

Polydimethylsiloxane membranes (~4.5 cm x ~4.5 cm; thickness = 70 μm) were punched with 1 mm diameter holes that were interspaced throughout the membrane (Fig. 1). Some of them were plasma polymerised with either acrylic acid or allylamine monomers to create thin hydrophilic layers of poly(acrylic acid) (AcA) or polyallylamine (AlA) coatings respectively (Altrika Ltd., UK). Fibrin/alginate porous hydrogels (Smart Matrix®) were manufactured from bovine fibrinogen using a foam-based method. Further chemical cross-linking with glutaraldehyde and freeze/drying of the structure produced a ~2 mm thick white sheet that was 80-90% porous with interconnected pores in the ideal range for cell infiltration and skin regeneration[29] (Fig. 1B). For manufacturing the hybrid two-component scaffold, the fibrin/alginate foam was cast on top of the Sil membranes prior to chemical cross-linking and freeze-drying steps. Sil membranes were slightly smaller (~4.5 cm x ~4.5 cm) than the fibrin/alginate hydrogel (~5 cm x ~5 cm) to be better able to observe the interface between the components (Fig. 1B).
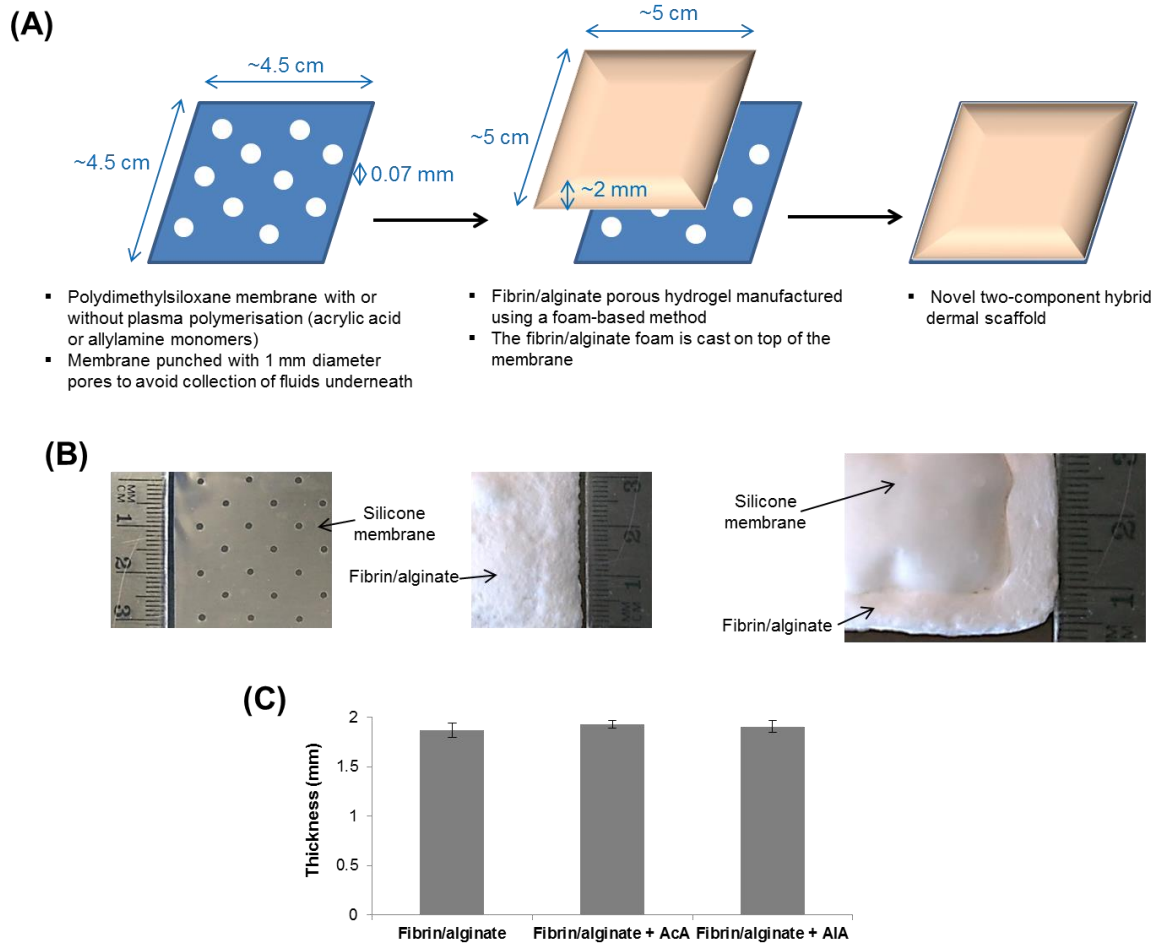
Figure 1. A) Scheme of the novel two-component hybrid dermal scaffold. B) Macroscopic photos of the different materials and hybrid scaffolds. C) Thickness of scaffolds presented as average ± standard deviation.

2.2 Thickness of scaffolds

Thickness of the different scaffolds was measured using a digital caliper. Scaffolds were held with forceps, the digital caliper was zeroed, and the outside jaws of the digital caliper adjusted to the edges of the scaffold, placed parallel to the jaws. Thickness was read in mm. Thickness of scaffolds was measured over 3 different randomly selected locations across the scaffold. Results were presented as average ± standard deviation.

2.3 Scanning electron microscopy (SEM)

Three scaffold per type of Sil membrane (manufactured in different batches) were imaged by SEM. Freeze/dried scaffolds were mounted on stubs, gold sputtered coated (Agar Auto Sputter Coater, Agar Scientific) and the cross-section and surface viewed (FEI Inspect F, Oxford Instruments, Oxford, UK).

2.4 Confocal scanning laser microscopy

The 3D structure of the scaffolds was examined by confocal scanning laser microscopy using a Leica DM IRE2 confocal microscope. Since SEM showed no structural variations across the different batches, 1 scaffold per type of Sil membrane from 1 batch was used. 5 mm x 5 mm pieces were cut from 3 different randomly selected locations across the scaffold. The auto-fluorescence of the scaffolds was detected using the 405 nm scanning laser. A total of 106 images were taken for Sil-AcA (9.7 μm step size), 91 images for Sil-AlA (9.7 μm step size) and 234 images for fibrin/alginate scaffold (Smart Matrix®) (5 μm step size) through the depth of the scaffolds. The depth of the z-stack was 1.02 mm for Sil-AcA, 837.2 μm for Sil-AlA and 1.17 mm for the fibrin/alginate scaffold. The confocal 3D z-stacks were processed using the Leica confocal software into maximum projection of the entire z-stack.

2.5 Pore size distribution

Pore size of the scaffolds was quantified from SEM images at 100X magnification, using ImageJ software (1.47v). The length of the scale bar on the SEM images was calculated and the distance in pixels was converted into the desired unit of length. Once the distance was set, the widest diameter of the pore was calculated and recorded. Pore size distribution was graphically represented by calculating the percentage of pore frequency over each scaffold. As with confocal microscopy, 1 scaffold per type of Sil membrane from 1 batch was used, with scaffolds cut into 5 mm x 5 mm pieces from 3 different randomly selected locations across the scaffold and one 100X image per location analysed.

2.6 Rheology

For this study we used a Kinexus Rheometer (Malvern Instruments, UK) in an oscillatory mode. From each dermal scaffold 4 cm x 4 cm samples were cut (n=3 per type of Sil membrane) and placed between two 20 mm diameter parallel plates (gap between plates=0.3 mm). The sample was hydrated and an integrated temperature controller was used to maintain the temperature of the sample stage at 20°C. A combined measurement including an 'amplitude sweep' and a 'frequency sweep' was carried out on each sample. The 'amplitude sweep' was performed by applying controlled stresses that were linearly increased from 0.1 to 10 %. Strains corresponding to the stresses were recorded. The oscillatory frequency was maintained at 1 Hz. The maximum strain within the linear viscoelastic region (LVER) was chosen from the 'amplitude sweep'. Log G′ or Log G″ was plotted against strain to obtain a rheological spectrum.

2.7 Cell culture

Cell experiments were performed using subcultures established from frozen stocks of primary normal human dermal fibroblasts (pnHDF), which were isolated from samples of normal human skin, obtained with donor consent and approved by local ethics committee. pnHDF cultures were maintained in Dulbecco's modified Eagle's medium (DMEM, 31885-023, Gibco, Paisley, UK) supplemented with 10 % fetal bovine serum (10270-106, Gibco, Paisley, UK), 100 U/ml Penicillin-Streptomycin (15140-122, Gibco, Paisley, UK), and 200 µM L-glutamine (25030-024, Gibco, Paisley, UK) at 37^0C with 5% CO_2. Cell morphology was routinely monitored by phase-contrast-light microscopy, medium was changed every 3-4 days and cells were passaged once they reached confluence. Cells were used at passages 5 or 6.

2.8 Cell seeding onto scaffolds

Scaffold were cut into 6 mm diameter discs and sterilised with 70 % IMS, washed with PBS (14190-094, Gibco, Paisley, UK) and tightly placed in a flat bottomed-96 well plate. The scaffolds were seeded with either 2.5×10^5 (live/dead and alamarBlue® assays) or 5×10^5 (histology and electron microscopy) pnHDF in 50 µl medium. After seeding, 200 µl of supplemented DMEM was added per well and the plate was incubated for 2 hours at 37^0C with 5% CO_2 to allow cells to settle onto scaffold discs. pnHDF seeded scaffold discs were transferred into a 12 well plate after incubation and covered with 2 ml of supplemented DMEM per well and cultured over a 7 day period at 37^0C with 5% CO_2.

2.9 Live/dead assay

Seeded scaffolds were assessed for cell incorporation and viability using Live/Dead cell staining according to the manufacturer's guidelines (Sigma), wherein live cells fluoresce green and dead cells fluoresce red. Briefly, scaffolds were washed in PBS prior to staining with the live/dead staining solution and then the staining procedure was performed in the dark for 30 minutes at 37°C and 5% CO_2. Live and dead cells were visualized by fluorescence imaging and confocal microscopy (Leica DM IRE2 confocal microscope).

2.10 alamarBlue® activity assay

Seeded scaffolds were transferred to fresh 12 well plates before the assay to ensure that only the metabolic activity of cells in the scaffolds was measured. Each cell seeded scaffold was tested with 1 ml of a 10 % alamarBlue® (DAL1025, Invitrogen™, Paisley, UK) solution, made up in phenol free supplemented DMEM

(11880, Gibco, Paisley, UK) and incubated for 3 hours at 37^0C with 5% CO_2. The 1 ml test samples were placed into a cuvette (FB55147, Fisher Scientific, Loughborough, UK) and the absorbance at 570 nm was read, following the manufacturer's instructions, against air in a M550 double beam UV/ visible spectrophotometer (Spectronic Camspec Ltd, Garforth, UK). The absorbance at 600 nm of the phenol-free DMEM was read and subtracted from the test sample absorbance to obtain the final absorbance value.

2.11 Paraffin histology of cellularised scaffolds

Cellular ingress into the dermal matrices was assessed by histological processing of cellularised scaffolds and haematoxylin and eosin (H&E) staining of cross-sections. After 4 or 7 days in culture, cellularised scaffolds were fixed in 4% paraformaldehyde, embedded in paraffin and 4 µm thick sections were cut for H&E staining. Stained sections were observed under light microscopy (Zeiss Axiophot, Zeiss, Jena, Germany) and photographed with a DC200 Leica digital camera and IC50 software.

2.12 Field emission scanning electron microscopy (FESEM) of cellularised scaffolds

FESEM was carried out on cellularised scaffolds at the last time point (day 7) of cell culture to observe interaction of cell layers with the material. Seeded scaffolds underwent processing prior to being observed by FESEM. The samples were fixed in 2.5% glutaraldehyde (AGR1011, Agar Scientific and UK) overnight. The fixed samples were then washed with 0.1 M sodium cacodylate buffer solution (Agar Scientific, UK) and then stained with 1% Osmium tetroxide (75632, Sigma-Aldrich, UK) in 0.1 M sodium cacodylate buffer for 45 minutes. The samples were later washed with sodium cacodylate buffer and subsequently dehydrated with a series of industrial methylated spirit (IMS) (20% - 60%, increasing in 10% increments) and 90%, 96% and 100% ethanol. Finally, the samples were left inside a fume hood in 100% ethanol to dry overnight. The samples were mounted onto metal stubs, coated with gold and palladium using the Gatan (model 681) high resolution ion beam coater before being observed using the JEOL field emission scanning electron microscope (JSM-7401F).

2.13 Statistics

A one-way analysis of variance (ANOVA) with a Holm-Sidak post-hoc analysis was carried out using Sigma Stat 3.5 software. A p value of < 0.05 was considered as a significant result.

3. Results and Discussion

3.1 Manufacturing and Characterization of Two-Component Hybrid Scaffolds

3.1.1 Macroscopic Appearance, Peel Test and Scaffold Thickness

Two-component hybrid scaffolds were manufactured by casting the fibrin/alginate foam on top of different Sil membranes (native or plasma polymerised with either acrylic acid or allylamine monomers) and were crosslinked with glutaraldehyde. The cross-linked composite was freeze-dried and further tested for structural, mechanical and cellular properties. Figure 1B shows that the scaffolds were macroscopically white and homogenous. At the end of the freeze-drying process, native Sil did not attach to the fibrin/alginate layer and was peeled off easily by manual peeling (Fig. 1B). This observation agreed with our previously published results using a novel immuno-based assay suggesting weaker binding between native Sil and fibrinogen that can be attributed to the hydrophobic nature of the Sil polymer.[31] However, the combination of plasma polymerized Sil and fibrin/alginate formed a stable structure with the components attached to each other. In fact, it was not possible to detach the derivatised Sil membranes from the fibrin/alginate layer by manual peeling, demonstrating that the plasma polymerised Sil membranes firmly anchored to the fibrin/alginate component. This could be due to the hydrophilic plasma polymerized layer deposited on the Sil surface.[28] Furthermore, no air pockets between the plasma polymerised Sil membranes and the fibrin/alginate components were observed, suggesting uniform binding between the two components. Based on the peel test and the macroscopic observations, and following our design criteria, scaffolds made with native silicone were ruled out as unsuitable for the intended purpose.

We also tested whether the addition of a Sil membrane would affect the thickness of the fibrin/alginate component which would not be desirable. The fibrin/alginate component (Smart Matrix®) has a thickness of ~2 mm ideal for a dermal scaffold since human dermis is 1.5-3 mm thick.[32] Our results showed that the addition of a Sil membrane, which was 0.07 mm thick, did not significantly affect scaffold thickness (Fig. 1C), in accordance with our outlined design criteria.

3.1.2 Structural Characterization

SEM was used to investigate the attachment and integration of the two components of the hybrid scaffolds. Images obtained by SEM analysis show a scaffold composed of two layers: a dense plasma polymerised Sil layer attached to a porous fibrin/alginate layer (Fig. 2). Binding between the polymerized Sil layer and

fibrin/alginate layer seemed uniform for both the composites. As previously reported, one of the main features of the fibrin/alginate dermal scaffold Smart Matrix® is the presence of both nano-fibres and nano-pores, thus resembling the natural extracellular matrix (ECM) which cells are exposed to *in vivo*.[29,33] SEM suggests that these nano-features are still present in the two-component hybrid scaffolds (Fig 2, images at 5000X, far right column).
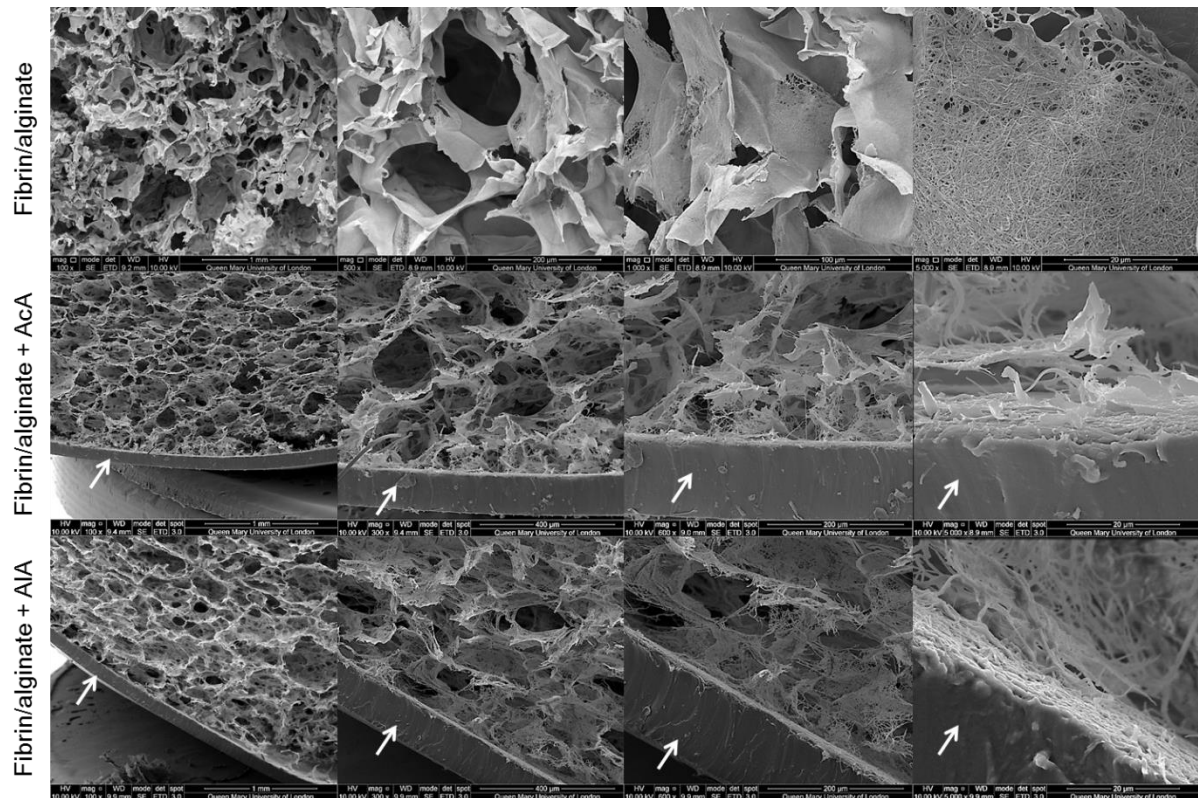

Figure 2. Representative SEM images of scaffolds. White arrows point at the silicone membrane. Scale bars left to right are: Fibrin/alginate, 1 mm / 200 μm / 100 μm / 20 μm; Fibrin/alginate + AcA, 1 mm / 400 μm / 200 μm / 20 μm; Fibrin/alginate + AlA, 1 mm / 400 μm / 200 μm / 20 μm. Images at 5000X (20 μm scale bar, far right column) show nano-pores and nano-fibres.

Confocal microscopy showed no qualitative differences in terms of surface topography between the fibrin/alginate scaffold and the two-component hybrid ones (Fig. 3). Confocal microscopy images also showed consistent results in terms of structure for the 3 scaffolds: all scaffolds presented open and interconnected porous structures with micro-pores in a range of sizes.
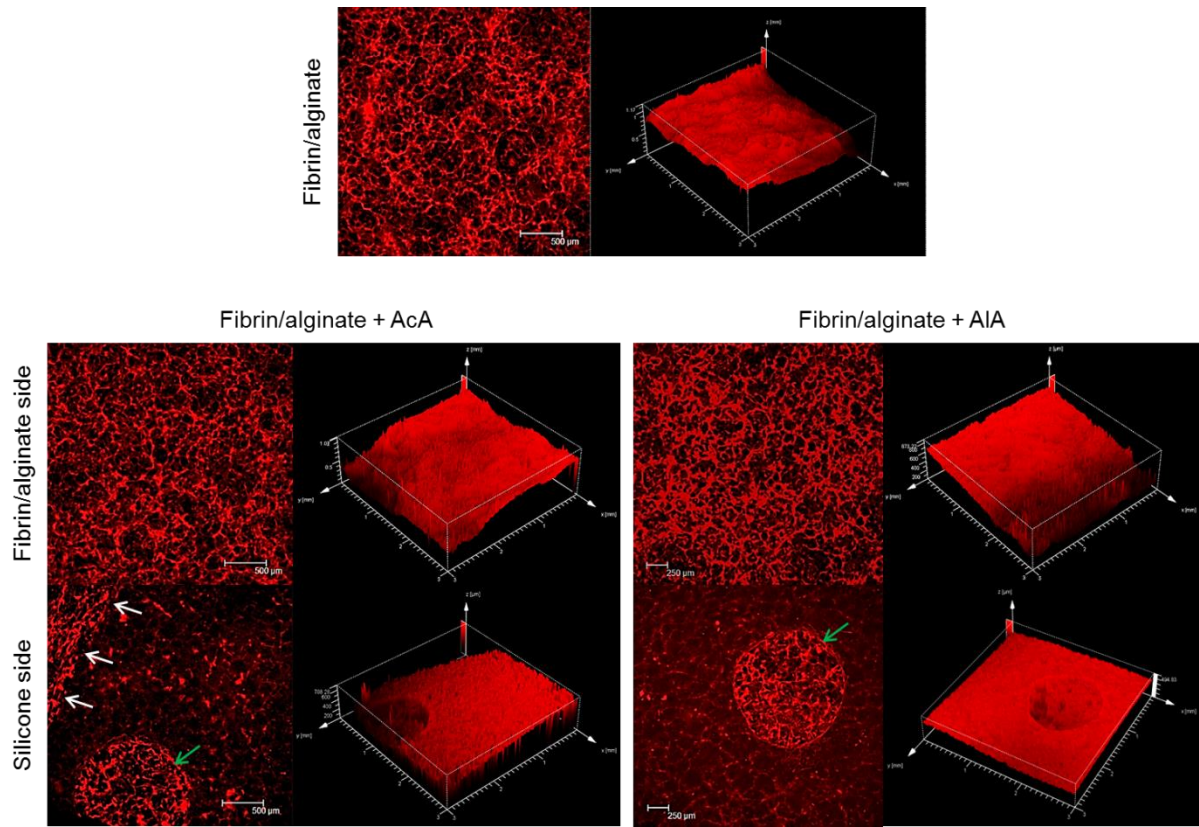
Figure 3. 3D confocal z-stacks of scaffolds. Green arrows point at 1 mm pores present in the silicone membranes. White arrows point at the edge between the silicone membrane and the fibrin/alginate component. Images on the right show surface topography graphs of the scaffolds.

Pore size distribution data showed very similar patterns for the 3 scaffolds: all had the majority of their pores in the range of 0-150 μm (Fig. 4). The literature refers to 20-125 μm as the ideal pore size range for skin regeneration while 10-110 μm is considered the ideal pore size range for cell infiltration.[34] Moreover, having a distribution of pore sizes that represents the actual *in vivo* scenario found in native tissue is important since cells in the body are in contact with a layer of tissue that possesses different pore sizes.[35]
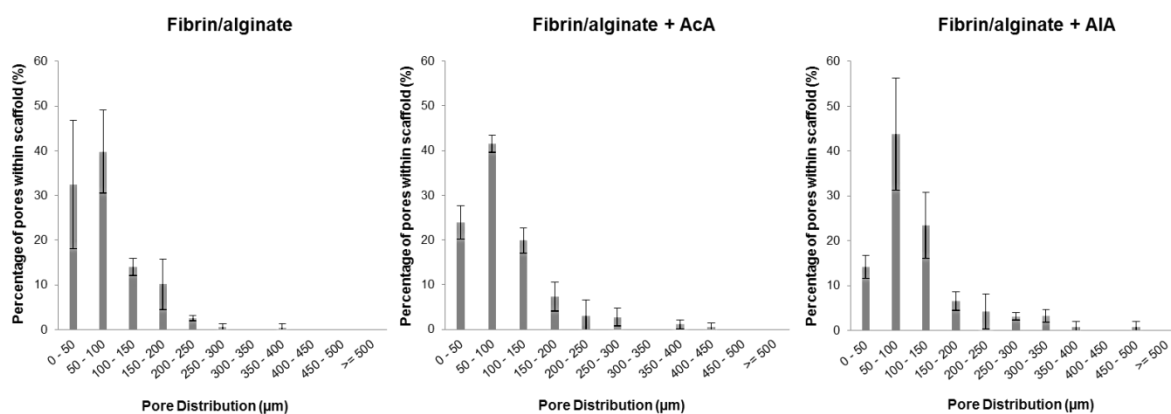
12

Figure 4. Pore size distribution in scaffolds. Results display average ± standard deviation.

Results from the structural characterisation were very encouraging since one of the essential points in the design criteria of this study was to keep the open and interconnected porous structure of the fibrin/alginate component intact as our previous work has shown that the structure is ideal for skin regeneration.[29] The next step of our study was to carry out rheological analysis of the hybrid scaffolds.

3.1.3 Rheology

As mentioned in our introduction, pressure sores are localised injuries affecting the skin and/or underlying tissue usually occurring over a bony prominence.[4] They happen as a result of pressure, shear and/or friction.[4] Limited literature exists regarding quantification of these forces, with interface pressure being the main focus of research probably due to being easier to assess compared to shear and friction. Interface pressure is defined as the perpendicular force applied per unit of area between the body and the support surface.[4] No quantitative data for pressure existed until Kosiak published in 1959 and 1961 his canine and rat experiments, which involved loading tissues with known pressures for specific durations with histology used to assess tissue viability: damage was observed in tissues subjected to as little as 8 kPa for only one hour.[36,37] More recent mean peak interface pressure values were reported by Peterson and colleagues: 8.6 to 17.9 kPa depending on position and patient type (at-risk or non-disabled).[4] Values for shear forces measured at 5 specific sites in the body were reported by Mimura *et al*., where mean values ranged between ~2.5 to ~22 N.[38] The general consensus is that shear and pressure act in conjunction to produce the damage to skin and/or underlying tissues that results in a pressure sore. We previously reported the magnitude of the shear or storage modulus G' for Smart Matrix® (average ± standard deviation = 8.26 ± 1.20 kPa),[29] which based on the values found in the literature for

13

interface pressure and shear would suggest that Smart Matrix® would not be strong enough to resist these forces. Hence, the aim of this work to combine it with a silicone membrane.

Various properties of silicones make them favourable for biomedical uses, especially for wound dressings, including low liquid surface tension, high permeability, pressure-sensitivity, mechanical resistance and ease of sterilisation.[39] Moreover, there are several documented cases of using silicone to enhance the mechanical properties of more fragile biomaterials, especially in the case of wound dressings.[40-44] As an example, Pires and Moares demonstrated the enhanced tensile strength and flexibility of chitosan-alginate membranes following incorporation of the liquid silicone rubber Silpuran® 2130 A/B.[40] This may be attributed to several factors including cross-linking of the silicone polymer chains at various points in the chitosan-alginate membrane to form a more resistant structure.[40]

In our study, the mechanical properties of the scaffolds were investigated by rheology, a branch of engineering that studies the viscoelastic properties (both solid and fluid) of materials as well as biological tissues.[29,45,46] Skin tissue has been described as a viscoelastic solid as under low magnitude oscillatory shear, as used in this study, its behaviour is primarily of an elastic nature.[45] Rheological analysis showed that the hybrid scaffolds had significantly higher shear and viscous moduli (G' and G'' respectively) than the original Smart Matrix® fibrin/alginate scaffold (Fig. 5). The shear or storage modulus G' is related to elasticity and is an indication of how the material stores energy which can be re-used in the form of elastic deformation. Therefore, G' relates to the solid characteristics of the material.[45-47] In our study, a higher G' for the hybrid scaffolds means that they have a higher strength compared to the fibrin/alginate scaffolds.[47] Moreover, the hybrid scaffolds manufactured using Sil plasma polymerised with acrylic acid monomers had higher G' and G'' than scaffolds manufactured with Sil plasma polymerised with allylamine monomers, suggesting that hybrid scaffolds with a membrane of Sil plasma polymerised with acrylic acid monomers would have a higher strength than hybrid scaffolds with a membrane of Sil plasma polymerised with allylamine monomers. This could be due to increased binding strength of fibrinogen to poly(acrylic acid) surfaces compared to polyallylamine surfaces.[28] However, these differences were not significant. Furthermore, for all scaffolds G'>G'' suggesting an elastic behaviour (solid) rather than viscous (fluid), also confirmed by the phase angle values which were closer to 0° (typical of elastic materials) than to 90° (typical of viscous materials).[45-47] Therefore, the scaffolds from this study could be described as viscoelastic solids, like skin tissue.

In summary, the rheology results show that by adding a silicone membrane to the original fibrin/alginate scaffold (Smart Matrix®) the resulting two-component scaffolds are more robust and therefore, would be more suitable for application in the treatment of pressure sores compared to Smart Matrix®. The concept of the backing membrane is to protect the protein scaffold from tearing when placed on difficult wounds on the lower back, buttocks or at the stump-socket interface, all areas which are subjected to high pressure, shear and/or friction.
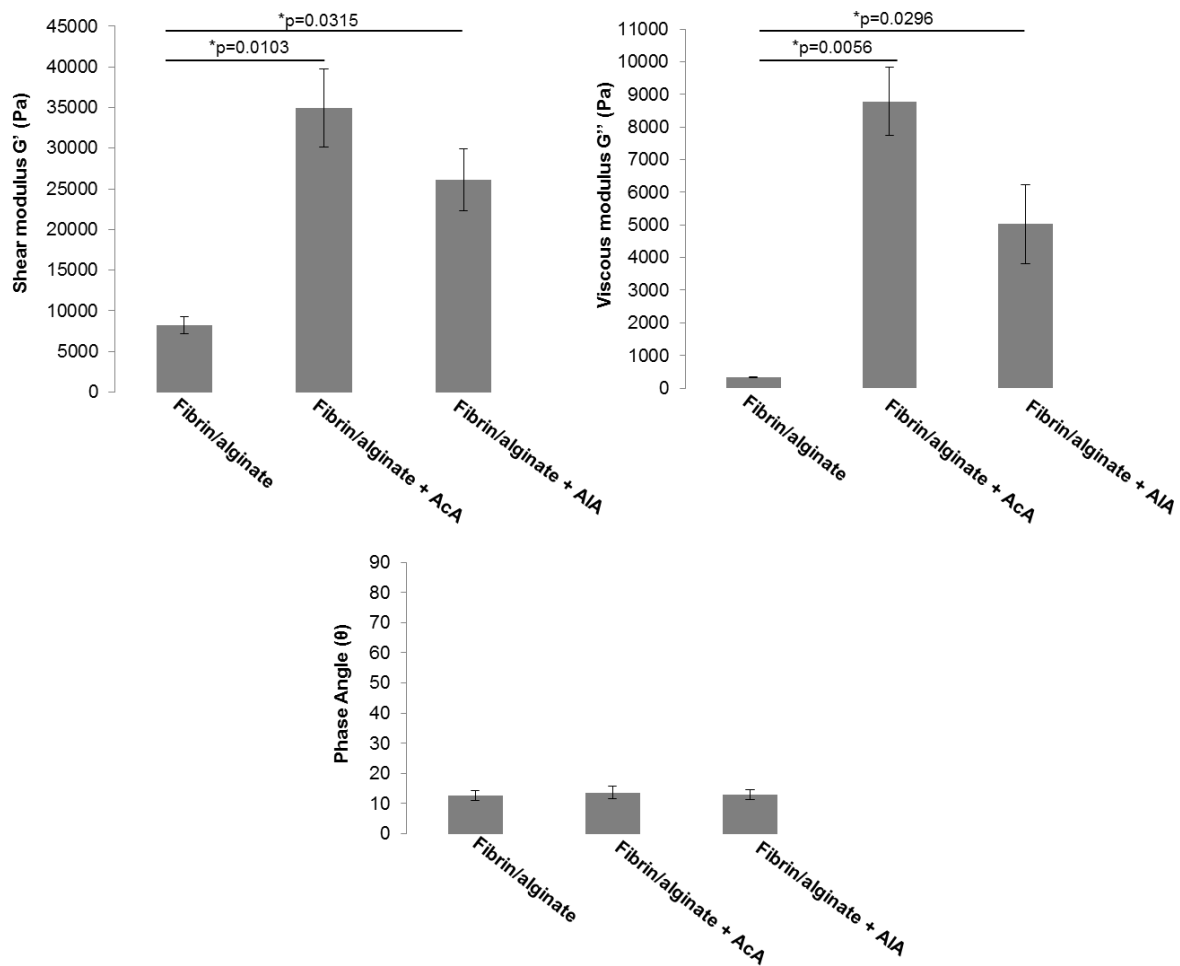

Figure 5. Rheological characterisation of scaffolds. Results display average ± standard deviation.

3.2 *In vitro* Cell Studies

Scaffolds for tissue repair and regeneration are used as 3D structural templates to support the adhesion, proliferation, differentiation and migration of cells. Therefore, before implanting scaffolds into hosts it is essential to demonstrate their biocompatibility *in vitro*. In our previous studies, *in vitro* cell work has been carried out on the individual components of the novel hybrid scaffold designed in this study: the fibrin/alginate matrix (Smart Matrix®) and the plasma polymerised Sil layers.[28-30] In this study, *in vitro* cell work on the two-component hybrid composite scaffold was carried out using primary human dermal fibroblasts, the main cell type found in the dermis.[48] Cell viability and growth were analysed by live/dead and metabolic (alamarBlue®) assays. Since the original fibrin/alginate Smart Matrix® has shown rapid infiltration of cells,[29,30] cell ingress into the scaffolds was also evaluated using histological processing and H&E staining. Finally, FESEM was used to investigate integration of cells with the material.

3.2.1 Cell Viability and Growth

Results showed that cells remained viable and proliferated through the culture period (Fig. 6). Metabolic activity was significantly higher on day 7 than on day 2 for all scaffolds (Fig. 6A), suggesting significant cell proliferation on the three scaffolds. Moreover, no significant differences were observed between the three scaffolds at any of the time points (Fig. 6A). These results suggest that cell viability and proliferation are not affected by addition of a silicone membrane.
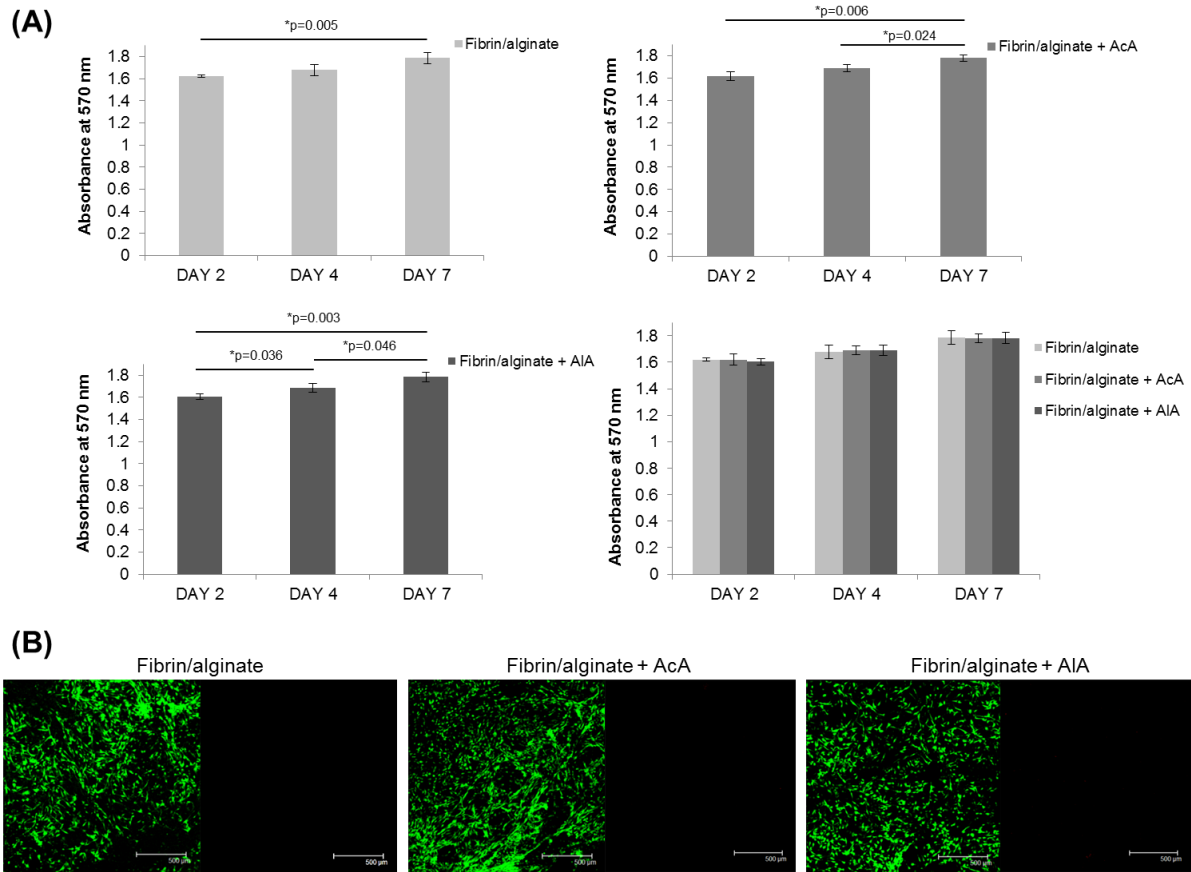
Figure 6. A) alamarBlue® metabolic assay over 7 days of culture. B) live/dead assay on day 7 showing viable cells on the three scaffolds: green colour (left) indicative of live cells and red colour (right) indicative of dead cells (scale bar = 500 μm).

3.2.2 Cell Ingress

Once a dermal scaffold is implanted, cells from the surrounding uninjured skin tissue migrate into the scaffold, proliferate, and start laying down a temporary collagen type III-rich ECM that will be later remodelled into a stronger collagen type I-rich ECM by matrix metalloproteinases that are secreted by fibroblasts, macrophages and endothelial cells.[49] Infiltration of cells into the scaffold is therefore critical for a successful outcome. Our previous research has suggested a high influx of cells into Smart Matrix®,[29,30] thus we wanted to determine whether the addition of a silicone membrane would affect cell infiltration into the fibrin/alginate component.

Our results showed that cell infiltration into the hybrid scaffolds was very similar to the fibrin/alginate scaffold (Smart Matrix®), with cells populating the entire depth of the scaffolds after 4 days in culture (Fig. 7A). Higher magnification photos showed cells attached to the fibres of the fibrin/alginate component (Fig. 7B).
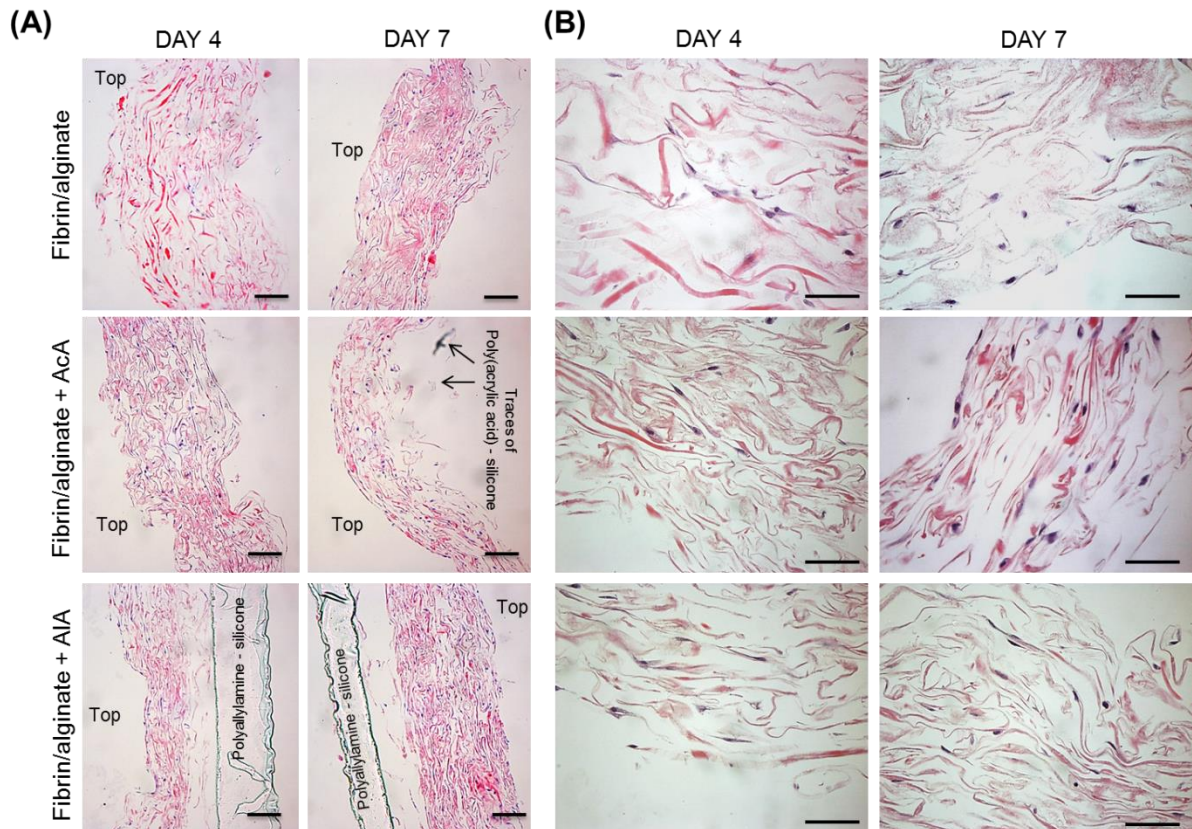

Figure 7. Paraffin histology and H&E staining of seeded scaffolds at days 4 and 7 of culture. Fibrin/alginate matrix appears pink while cells are stained in purple colour. A) Scale bar = 100 µm and B) scale bar = 50 µm. The silicone membrane plasma polymerised with acrylic acid monomers came off after the histological processing and only traces of it could be seen. For the hybrid scaffold manufactured using polyallylamine silicone, the membrane was still present after the histological processing, although photos show that it was not firmly bound to the fibrin/alginate component.

3.2.3 Cell Integration

To observe the interaction of pnHDF with the hybrid scaffolds, FESEM was used. Hybrid scaffolds seeded with pnHDF were subjected to FESEM at the last time point (day 7 of culture) and compared to the control fibrin/alginate scaffolds without any Sil membrane. The FESEM images showed good attachment of cells in all samples with cells embedded within the matrix (Fig. 8). These results demonstrate good interaction of dermal fibroblasts, the main cell type found in the dermis layer of skin,[48] with the fibrin/alginate component of the hybrid scaffolds, which is essential for dermal repair.
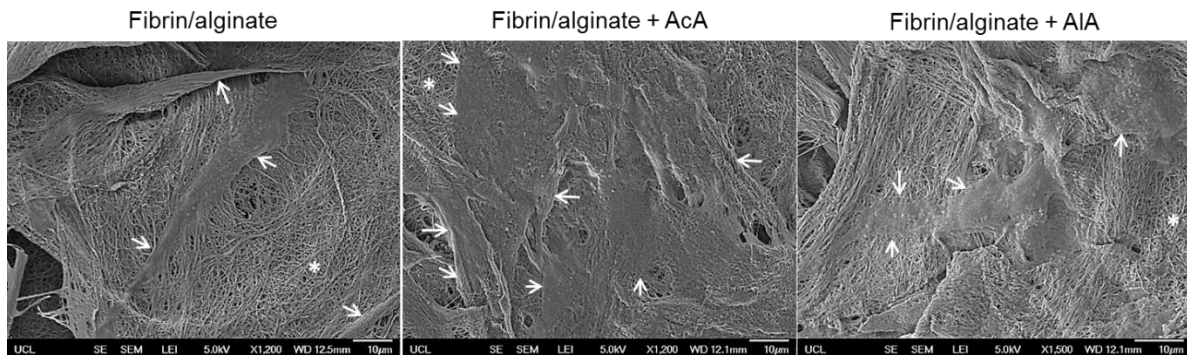

Figure 8. FESEM images of seeded scaffolds at day 7 of culture. *shows the nano-fibres and nano-pores present in the fibrin/alginate matrix. White arrows point at cells which are seen embedded in the matrix. For all images scale bar = 10 µm.

Results from the *in vitro* cell studies showed that addition of a plasma polymerised Sil membrane to the fibrin/alginate scaffold did not have an effect in terms of cell viability, growth, ingress, and integration, in accordance with our design criteria. Moreover, results from our work pose the question of which plasma polymerised Sil membrane would be best for the two-component hybrid scaffold: poly(acrylic acid) or polyallylamine coating. The only difference found between both membranes was in the rheological characterisation; the hybrid scaffold manufactured with a poly(acrylic acid)-Sil membrane was found to be stronger than the one manufactured with a polyallylamine-Sil membrane (Fig. 5), although this difference was not significant. We believe that further *in vivo* work in a suitable animal model could help to answer this question. The Sil membrane is only intended as a temporary cover to protect the fibrin/alginate component from

the forces experienced in pressure ulcers. Therefore, the Sil membrane will be ultimately removed. *In vivo* work will also help to answer the question regarding removal of the membrane after implantation of the hybrid scaffold, since the fibrin/alginate component will start degrading *in vivo* as new dermal tissue is formed.

The main strategy currently used in the treatment of pressure sores is relief of pressure using specialist support surfaces together with management of the wound environment using wound dressings. Moreover, pain management, optimising circulation/perfusion, patient education, nutrition, and the treatment of infection are applied. Signs of healing are expected within two weeks of initial treatment. However, in many instances improvement may not occur and deterioration is observed.[50] Therefore, tissue engineering strategies have been explored as an alternative. Several tissue-engineered scaffolds have been applied for the treatment of pressure sores. Different types of tissue-engineered skin substitutes exist (animal derived, cellular and acellular) and they all offer advantages and disadvantages. Animal derived skin substitutes, i.e. OASIS Wound Matrix® (decellularised porcine jejunal submucosa) or MatriStem® UBM (porcine bladder-derived extracellular matrix), have been used to treat pressure sores as well as other chronic wounds such as venous and diabetic ulcers. The reported disadvantages of these products are rejection (main issue), infection and disease transfer.[3,51,52] Cellular skin substitutes such as Apligraf® (composite bilayered product consisting of living keratinocytes and fibroblasts derived from neonatal human foreskin in a bovine collagen gel matrix) or Dermagraft® (cryopreserved allogenic human neonatal foreskin fibroblast-derived bioabsorbable dermal matrix) have been used to treat chronic ulcers. However, these products are complex composites consisting of living cells which adds to the biomaterials high cost, manufacturing difficulty and limited shelf-life.[53-55] Acellular skin substitutes eliminate the complexity and limited shelf-life of cellular products. The most commonly used acellular substitute is Integra®, which is composed of a temporary silicone epidermal substitute over a dermal scaffold made of bovine collagen type I and chondroitin-6-sulphate from shark cartilage.[29] Integra® has been used in the treatment of pressure sores with reported wound closure. However, the main disadvantage of using Integra® is a risk of infection due to the collection of fluid underneath the silicone layer.[8,56] Our proposed hybrid scaffold has a punched silicone membrane to allow fluid flow thus potentially eliminating the problems previously reported with Integra®. Another disadvantage of using Integra® is that it is not easily biodegradable and has been reported to stay in the body for up to 2 years after implantation, with an associated risk of inflammatory reaction.[57,58] An earlier study by our group showed that the fibrin/alginate matrix degrades faster than Integra®.[29] Faster degradation of our hybrid scaffolds can be argued to be a disadvantage in a chronic

environment, but the timeline of degradation can be optimized by varying different parameters depending on the depth of injury. Finally, our proposed hybrid scaffold is designed to address issues currently observed with the major skin substitutes used in chronic conditions and therefore, we believe that it could offer advantages over existing products.

4. Conclusion

The aim of our study was to design a novel two-component hybrid scaffold using the fibrin/alginate porous hydrogel Smart Matrix® combined to a backing layer of plasma polymerised polydimethylsiloxane membrane to make the fibrin-based dermal scaffold more robust for the treatment of the clinically challenging pressure sores. Plasma polymerization was used to add specific functional groups to the otherwise bioinert Sil: acrylic acid or allylamine monomers were used to generate thin layers rich in carboxyl (-COOH) and amine ($-NH_2$) groups making the Sil surface highly branched and cross-linked to facilitate the immobilization of biomacromolecules (fibrin in this study). A design criteria was established, according to which the Sil membranes were punched to avoid collection of fluid underneath which could lead to oedema *in vivo*. The fibrin/alginate porous hydrogel (Smart Matrix®) is manufactured using a foam-based method, so for manufacturing the hybrid scaffolds the fibrin/alginate foam was cast on top of the Sil membranes. Manual peel test showed that native silicone did not attach to the fibrin/alginate component while the plasma polymerised silicone membranes were firmly bound to the fibrin/alginate matrix. Structural characterisation showed that the fibrin/alginate matrix was intact (open and interconnected porous structure with micro-pores in an ideal range for cell infiltration and skin regeneration) after addition of the Sil membrane, in agreement with our design criteria. Rheology results showed that by adding a Sil membrane to the original fibrin/alginate scaffold (Smart Matrix®) the resulting two-component scaffolds had a significantly higher shear or storage modulus G' making them stronger than the fibrin/alginate scaffold, and therefore, would be more suitable for the treatment of pressure sores in comparison to Smart Matrix® alone. *In vitro* cell studies showed that dermal fibroblasts remained viable, proliferated and infiltrated the scaffolds during the culture period. Our results show that the design of a novel two-component hybrid dermal scaffold was successful according to our proposed design criteria. To the best of our knowledge, this is the first study that reports combination of a fibrin-based scaffold with a plasma-polymerised silicone membrane.

Acknowledgements

References

[1] R.G. Frykberg, J. Banks, *Adv. Wound. Care.* **2015**, 4(9), 560.

[2] S. R. Baker, M. C. Stacey, G. Singh, S. E. Hoskin, P. J. Thompson, *Eur. J. Vasc. Surg.* **1992**, 6, 245.

[3] N. S. Greaves, S. A. Iqbal, M. Baguneid, A. Bayat, *Wound. Repair. Regen.* **2013**, 21, 194.

[4] M. J. Peterson, N. Gravenstein, W. K. Schwab, J. H. van Oostrom, L. J. Caruso, *J. Rehabil. Res. Dev.* **2013**, 50(4), 477.

[5] P. Laszczak, L. Jiang, D.L. Bader, D. Moser, S, Zahedi, *Med. Eng. Phys.* **2015**, 37(1), 132.

[6] B. Lineham, P. Harwood, P. Giannoudis, *Prosthet. Orthot. Int.* **2015**, 39(2), 157.

[7] Health Quality Ontario. *Ont. Health. Technol. Assess. Ser.* **2009**, 9(3), 1.

[8] K. S. Vyas, H. C. Vasconez, *Healthcare* **2014**, *2*, 356.

[9] S. P. Zhong, Y. Z. Zhang, C. T. Lim, *Nanomed.Nanobiotechnol* **2010**, 2, 510.

[10] V. C. van der Veen, M. B. A. van der Wal, M. C. E. van Leeuwen, M. M. W. Ulrich, E. Middelkoop, *Burns* **2010**, 36, 305.

[11] V. W. Wong, G. C. Gurtner. *Exp. Dermatol.* **2012**, 21(10), 729.

[12] L. S. Nair, C. T. Laurencin, *Prog. Polym. Sci.* **2007**,32, 762.

[13] I. V. Yannas. Classes of materials used in medicine: natural materials, In *Biomaterials Science: An Introduction to Materials in Medicine.* 2nd Edition; Ratner, B. D., Ed.; Elsevier Academic Press. **2004**. pp 127–36.

[14] M. R. Badrossamay, K. Balachandran, A. K. Capulli, H. M. Golecki, A. Agarwal, J. A. Goss, H. Kim, K. Shin, K. K. Parker, *Biomaterials* **2014**, 35, 3188.

[15] Hu X, Cebe P, Weiss A S, Omenetto F and Kaplan D L 2012 Protein-based composite materials *Mater. Today* 15 208–15.

[16] K. Mojsiewicz-Pieńkowska, M. Jamrógiewicz, K. Szymkowska, D. Krenczkowska. *Front. Pharmacol.* **2016**, 7, 132.

[17] L. Filipponi, P. Livingston, O. Kašpar, V. Tokárová, D. V. Nicolau. *Biomed. Microdevices.* **2016**, 18(1), 9.

[18] B. A. Evans, J. C. Ronecker, D. T. Han, D. R. Glass, T. L. Train, A. E. Deatsch. *Mater. Sci. Eng. C. Mater. Biol. Appl.* **2016**, 62, 860.

[19] F. H. Lahey. *Ann. Surg.* **1946**, 124, 1027.

[20] A. Tabor, R. Diller, J. Chinn. *Silicone valley: a biomaterial for med-tech*. Medical Device Developments Magazine **201**3 [ONLINE] http://www.medicaldevice-developments.com/features/featuresilicone-valley-biomaterial-med-tech/. [Accessed 10 August 2016].

[21] J. M. Curtis, A. Colas. Dow Corning(R) Silicone Biomaterials: History, Chemistry & Medical Applications of Silicones, In *Biomaterials Science: An Introduction to Materials in Medicine*, 2nd Edition; Ratner, B. D., Ed.; Elsevier Academic Press. London, UK. **2004**. pp. 80-86, pp. 697-707.

[22] C. J. White, S. A. DiPasquale, M. E. Byrne. *Optom. Vis. Sci.* **2016**, 93(4), 377.

[23] M. Navarro, A. Michiardi, O. Castaňo, J. A. Planell. *J. R. Soc. Interface.* **2008**, 5, 1137.

[24] S. MacNeil. *Materials. Today.* **2008**, 11(5), 26.

[25] M. Notara, N. A. Bullett, P. Deshpande, D. B. Haddow, S. MacNeil, J. T. Daniels *J. Mater. Sci. Mater. Med.* **2007**, 18(2), 329.

[26] D. B. Haddow, D. A. Steele, R. D. Short, R. A. Dawson, S. MacNeil. *J. Biomed. Mater. Res. A.* **2003**, 64A, 80.

[27] B. Cao, S. Yan, K. Zhang, Z. Song, T. Cao, X. Chen, L. Cui, J. Yin. *Macromol. Biosci.* **2011,** 11**,** 970.

[28] V. Sharma, K. A. Blackwood, D. Haddow, L. Hook, C. Mason, J. F. Dye, E. García-Gareta. *Biochim. Open* **2015**, 1, 40.

[29] V. Sharma, N. Patel, N. Kohli, N. Ravindran, L. Hook, C. Mason, E. García-Gareta. *Biomed. Mater.* **2016**, 11, 055001.

[30] E. García-Gareta, N. Ravindran, V. Sharma, S. Samizadeh. J. F. Dye. *Biores. Open. Access.* **2013**, 2, 412.

[31] A. S. Mikhail, J. J. Ranger, L. Liu, R. Longenecker, D. B. Thompson, H. D. Sheardown, M. A. Brook. *J. Biomater. Sci. Polym. Ed.* **2010**, 21, 821.

[32] G. K Menon. *Adv. Drug. Delivery. Reviews.* **2002**, 54, S3.

[33] D. Singh, D. Singh, S. Zo, S. S. Han. *J. Biomed. Nanotechnol.* **2014**, 10(10), :3141.

[34] Y. Ikada. Tissue engineering: fundamentals and applications. **2011**. Academic Press. UK.

[35] Q. L. Loh, C. Choong. *Tissue. Eng. Part. B.* **2013**, 485.

[36] M. Kosiak. *Arch. Phys. Med. Rehabil.* **1959**, 40(2), 62.

[37] M. Kosiak. *Arch. Phys. Med. Rehabil.* **1961**, 42, 19.

[38] M. Mimura, T. Ohura, M. Takahashi, R. Kajiwara, N. Ohura. *Wound. Rep. Regen.* **2009**, 17,789.

[39] X. Thomas. Silicones in Industrial Applications: 17. Silicone in Medical Applications. In *Inorganic Polymers.* De Jaeger, R., Gleria, M. Eds. Nova Science Publishers, **2007**. Chapter 2.

[40] A. L. R. Pires, Â. M. Moares, *J. Appl. Polym. Sci.* **2015**, 132(12), 41686.

[41] H. Xie, W. Yang, J. Chen, J. Zhang, X. Lu, X. Zhao, K. Huang, H. Li, P. Chang, Z. Wang, L. Wang. *Adv. Healthc. Mater.* **2015**, 4(15), 2195.

[42] N. Vázquez, M. Chacón, Á. Meana, Y. Menéndez-Menéndez, A. Ferrero-Gutierrez, D. Cereijo-Martín, M. Naveiras, J. Merayo-Lloves. *Histol. Histopathol.* **2015**, 30(7), 813.

[43] J. Guthrie, R. Potter. *J. Wound. Care.* **2016**, 25(8), 465.

[44] J. Wasiak, H. Cleland. *B. M. J. Clin. Evid.* **2015**, pii: 1903.

[45] B. Holt, A. Tripathi, J. Morgan. *J. Biomech.* **2008**, 41(12), 2689.

[46] S. Saitoh, K. Sasaki, T. Nezu, M. Taira. *Dent. Mater. J.* **2010**, 29(4), 461.

[47] C. Helary, I. Bataille, A. Abed, C. Illoul, A. Anglo, L. Louedec, D. Letourneur, A. Meddahi-Pellé, M. M. Giraud-Guille. *Biomaterials.* **2010**, 31(3), 481.

[48] S. V. Nolte, W. Xu, H. O. Rennekampff, H. P. Rodemann. *Cells. Tissues. Organs.* **2008**, 187(3), 165.

[49] G. C. Gurtner , S. Werner, Y. Barrandon, M. T. Longaker. *Nature.* **2008**, 453(7193), 314.

[50] M.J. Westby, J.C. Dumville, M.O. Soares, N. Stubbs, G. Norman. *Cochrane. Database. Syst. Rev.* **2017**, 6:CD011947.

[51] E.N. Mostow, G.D. Haraway, M. Dalsing, J.P. Hodde, D. King. *J. Vasc. Surg.* **2005**, 41, 837.

[52] J. LeCheminant, C. Field. *J. Wound. Care.* **2012**, 21, 476.

[53] J.T. Trent, A. Falabella, W.H. Eaglstein, R.S. Kirsner. *Ostomy. Wound. Manage.* **2005**, 51, 38.

[54] A. Veves, V. Falanga, D. Armstrong, M. Sabolinski. *Diabetes. Care.* **2001**, 24, 290.

[55] W.A. Marston, J. Hanft, P. Norwood, R. Pollak. *Diabetes. Care.* **2003**, 26, 1701.

[56] H. Tchero, C. Herlin, F. Bekara, P. Kangambega, F. Sergiu, L. Teot. *Wound. Repair. Regen.* **2017**. DOI:10.1111/wrr.12554. Ahead of print.

[57] J.C. Jeng, P.E. Fidler, J.C. Sokolich, A.D. Jaskille, S. Khan, P.M. White, J.H. Street, T.D. Light, M.H. Jordan. *J. Burn. Care. Res.* **2007**, 28, 120.

[58] J.M. Anderson, A. Rodríguez, D.T. Chang. *Semin. Immunol*. **2008**, 20, 86.